ELSEVIER

Contents lists available at ScienceDirect

# Chemical Engineering Journal

journal homepage: www.elsevier.com/locate/cej



# Catalytically sustainable, palladium-decorated graphene oxide monoliths for synthesis in flow



Sajjad Ghobadi<sup>a,b</sup>, Michael B. Burkholder<sup>a</sup>, Sarah E. Smith<sup>a</sup>, B. Frank Gupton<sup>a</sup>, Carlos E. Castano<sup>b,\*</sup>

# HIGHLIGHTS

- Ethanol treatment improves graphene-based monolith's robustness in aqueous media.
- MW irradiation improves the catalytic activity but reduces robustness of monoliths.
- Flow synthesis lifetime of monolithic catalysts was 300% higher than packed beds.
- Monoliths cause no backpressure, hence improving the flow synthesis throughput.
- A 3D cm-scale map of Pd distribution in graphene monolith can be obtained by CT-scan.

#### ARTICLE INFO

# Keywords: Monolith Flow synthesis Catalyst CT-scan Esterification Freeze casting

#### ABSTRACT

Continuous flow synthesis is an essential route towards high throughput manufacturing of fine chemical and pharmaceutical products. The mentioned chemistries are often catalyzed by solid-supported catalysts via packed beds which are characterized by multiple issues such as high pressure-drops, micro channeling through the bed, and leaching of the metallic catalyst into the product stream. These issues lower the overall process efficiency. Three dimensional (3D) structures, known as monoliths, with high porosity and mechanical robustness, offer the ideal properties to be used macroscopic supports for metallic catalyst particles. This approach has shown to alleviate several known issues with catalyst packed beds effectively.

Herein centimeter-scale monolithic catalysts of palladium (Pd)-decorated, covalently-bonded graphene oxide (GO) layers have been prepared via a completely aqueous, one-pot system. These monolithic composite structures were designed for Suzuki cross-coupling reactions in flow. As highly engineered materials, monoliths' properties such as oxygen content and Pd catalyst ionic species were tuned via microwave irradiation and ethanol vapor reduction treatments. The optimal monolithic catalysts showed over 5 h of operational longevity in flow, which was 300% higher than the conventional Pd on GO catalyst packed beds. As a proof of concept, the monolithic catalyst was successfully used as a model structure for nondestructive X-ray CT-scan elemental and porosity mapping in the centimeter scale.

# 1. Introduction

Since the 19th century, catalysts have been actively utilized in a variety of processes [1]. These catalysts due to kinetic effects can accelerate the production of a certain product or efficiently generate energy by reducing the activation barrier of the reactions. The importance of catalyst development is highlighted by the tremendous amount of research being conducted to meet the rapidly growing demand for large quantities of synthetic products, improving reaction efficiency, and

catalyzing more difficult reactions [2].

Traditionally, many petrochemical and fine chemical industries use metal particles as their catalysts of choice for most catalyzed processes. Specifically, cross-coupling processes in the pharmaceutical industry have utilized selective transition metal catalysts [3,4]. Homogeneous metal compounds [5,6] are favored for such applications due to their durability and high activity. These homogeneous catalysts are usually expensive, require high catalyst loading, and are difficult to separate from products [7]. It is noteworthy that the metal impurities in

E-mail address: cecastanolond@vcu.edu (C.E. Castano).

<sup>&</sup>lt;sup>a</sup> Department of Chemical and Life Science Engineering, Virginia Commonwealth University, United States

<sup>&</sup>lt;sup>b</sup> Department of Mechanical and Nuclear Engineering, Virginia Commonwealth University, United States

<sup>\*</sup> Corresponding author.

pharmaceutical products are highly regulated by agencies such as the Food and Drug Administration (FDA) (e.g. 10 ppm limit for Palladium in Q3D Elemental Impurity Guidance for Industry [8]) making the separation of the metallic species from products a crucial and often costly issue.

Heterogeneous catalysis is one of the most effective ways to address these drawbacks. For example, the utilization of solid-supported catalysts not only provides ease of separation, it also reduces or eliminates the amount of metal contamination of the products [9–12]. Nevertheless, additional improvements are sometimes required for a solid-supported catalyst to be technically and financially feasible on a commercial level.

Overcoming the costs associated with solid-supported catalysts can be achieved by increasing the catalytic activity through synthesizing smaller metal particles on solid-supports. This approach results in increased active surface area to volume ratio. Another improvement pursued in solid-supported catalysis is to utilize an electrically conducting support for fast and low activation energy redox cycle of metal particles during catalysis. This goal has been achieved by using conducting and cheap supports (e.g. graphene [13–15], activated charcoal [16] and carbon black [17]).

One challenge that recently has received interest is to effectively implement the use of solid-supported catalysts in continuous or flow syntheses (e.g., catalyst packed bed reactor configuration) in petrochemical catalysis <sup>18</sup> and particularly, active pharmaceutical ingredients (APIs) [18,19]. As stated by Buchwald et al. has identified multiple difficulties to be addressed in flow synthesis, and importantly the implementation of solid-supported catalysts was listed as one of the top challenges in that framework [4]. Packed catalyst beds tend to have a high pressure-drop across the bed, flow channeling, or clogging, preventing their effective use and commercialization [20,21].

The high pressure-drop in flow synthesis can be a result of the solidsupported catalysts packing, which also reduces the available active sites and thus catalytic activity. Catalyst packing can also lead to accelerated deactivation [20]. Micro channeling of catalyst packed beds is another issue that prevents efficient catalysis as the reaction media can flow through these channels and interact less with the catalyst particles. In other words, the residence time as well as catalyst efficacy are both reduced [21].

Research efforts to address high pressure-drop and micro channeling of catalyst packed beds have been reported using various bottom-up assembly methods for large scale catalyst preparation. In Haswell and co-workers' study [22], sol-gel bottom-up assembly of silica nanoparticles led to formation of a robust macroscopic structure. A three-dimensional (3D) Pd/silica monolithic catalyst was synthesized by physically adsorbing palladium salt precursors on silica nanoparticles. The preparation process was then completed by calcination of the silica monoliths which ultimately resulted in improved catalyst performance in flow synthesis. However, the harsh and non-reproducible conditions of both sol-gel, as well as calcination processes, were among the main drawbacks of this approach.

In another study by Barbaro et al. [23], it was shown that a Pd@ sulfonated silica monolith was prepared as a catalyst for partial hydrogenation reactions. While the catalytic activity of the monolithic catalysts improved over four times in selectivity with respect to the two-dimensional Pd@silica, the catalyst preparation required the expensive commercial monolith and harsh functionalization treatment conditions thereof.

In a recent study by Minati and co-workers [24], graphene xerogels decorated with Pd was prepared via hydrothermal assembly methods and used as monolithic catalysts for catalytic dye (Rhodamine 6G) reduction. Empowered by its highly porous, yet sturdy structure, the monolithic catalyst was able to complete the reaction in half the conventional periods.

Modak et al., prepared Pd particles immobilized inside hollow n-doped carbon tubes with holes in their structure. These macroscopic 3D

supports were obtained through a top-down manufacturing process, during which highly cross-linked polymer tubes, as well as catalyst efficacy, in the presence of Pd (II) ions. They showed such high surface area macroscopic structures possess significantly improved catalytic activity over their conventional 2D solid-supported counterparts. Such structures' performance superiority was confirmed for Sonogashira and cyanation type C–C bond formation reactions as well as hydrogenation of nitrobenzene and compounds similar to their corresponding anilines [251].

Diaz-Marta and co-workers [26], prepared 3D printed  $SiO_2$  supports for Pd and copper (Cu) compartmentalized loading, leading to the preparation of monolithic catalysts. These multicomponent monolithic catalysts were able to work in tandem for a variety of cross-coupling reactions including Sonogashira, Suzuki, and Stille mechanisms. The authors mentioned the need to obtain a map of the macroscopic catalysts structures. Hence, time-of-flight secondary ions mass spectrometry (TOF-SIMS) was applied to obtain the map. However, the mentioned method, in addition to being expensive, only provides a distribution map in 2D, which lacks the desired information of metal particle distribution in the prepared 3D structure.

An optimized monolithic catalyst has been the main interest of the related research community. Achieving this will require a straightforward, efficient, and low-cost preparation method. Additionally, the catalyst sustainability and ultimate flow catalytic longevity of these engineered hybrid nanomaterials need to be systematically studied [27–30].

A rigorous study of 3D monolithic catalysts will require characterization of the pore structure on the macroscopic level. During multiple studies it was shown that the solvents and reagents are often entrapped within the nanoporous structure due to capillary conditions, making conventional porosity measurements ineffective. These problems have drawn the community's focus towards more facile nondestructive analytical techniques [31].

Recently there have been reports on using computer assisted tomography (CT-scan) scanning technique for evaluation of fillers and additive material orientations in polymer composites [32]. During these investigations, the contrast was obtained by the difference in the X-ray diffraction of fillers and polymer matrix layers. CT-scanning was then used to study the interior structure of the composites. However, since both the matrix and the additives are carbon-based, no elemental distinction could be obtained at larger than nanometer scales [33].

In Sheppard and co-workers' report, ceria-doped gold monolithic catalysts were also studied by micro-CT scan imaging giving micro-meter scale resolution of the structure [30]. The study showed nano-porous gold/ceria monolith can be effectively used for catalysis and process intensification. However, the tomographic 3D mapping technique utilized, was not able to provide a ceria distribution map within the gold monolith structure. Large-scale structural alterations that occurred during the catalytic performance were not characterizable using micro-CT scan tomography.

The present study first investigates a multi-step, all aqueous-phase assembly approach for preparation of palladium-decorated graphenebased monolithic catalysts for improved catalytic performance. Afterwards, investigations on a new monolithic catalyst characterization technique using nondestructive micro CT-scan tomography for elemental and porosity mapping on the centimeter-scale is presented. The robustness of these monoliths to withstand synthesis in flow conditions was pursued via GO interlayer esterification; followed by a GO ethanol vapor partial reduction. The monolith structure was systematically analyzed and characterized by electron microscopy, X-ray photoelectron spectroscopy, and X-ray diffraction. The catalytic longevity of the monolithic catalysts in flow packed bed configuration was tested using a model Suzuki cross-coupling reaction and compared to the 2D catalyst. The feasibility and utility of the micro-CT mapping on the monolith structures was investigated with emphasis on microporosity alterations as well as Pd distribution throughout the entire monolithic structure.

# 2. Materials and methods

# 2.1. Materials

Graphite flakes (> 325 mesh size), 4-bromotoluene, and palladium chloride were purchased from Alfa-Aesar (Haverhill, MA, USA). Sulfuric acid, nitric acid, dichloromethane, hydrogen peroxide, ethanol, polyvinyl alcohol (PVA) (99% hydrolyzed, MW. 8900–98000 g.mol<sup>-1</sup>), ascorbic acid, chloroform-D, and acetonitrile were purchased from Sigma-Aldrich (Saint Louis, MO, USA). Phosphoric acid, hydrochloric acid, and potassium carbonate were purchased from Fisher Scientific (Hampton, NH, USA). Sucrose, phenylboronic acid, and tetra-aminepalladium(II) chloride (Alfa Aesar, 99.9%), were purchased from Caisson Labs (Smithfield, UT, USA), Fluka (Muskegon, MI, USA), and Science Labs (USA), respectively. All the chemicals were used without further purification.

# 2.2. GO monolith preparation

Graphene oxide was synthesized from graphite flakes via a green iteration of Hummer's modified method as described elsewhere [34]. Briefly, graphite nanosheets were oxidized by using KMnO<sub>4</sub>,  $\rm H_2SO_4$ , and  $\rm H_3PO_4$  for 24 h, followed by dialysis in DI water until the GO mixture reached a pH of 5 and was then dried in a vacuum oven overnight. Once dried, the GO was dispersed in DI-water (5 mg/mL) by ultrasonication using an ultrasound bath (150 W, 100% amplitude, Branson\* 1800) for 7 h. Then, 2.5 mg sucrose and 0.25 mL of 1 wt/vol% aqueous solution of PVA (2.5 mg solid ca.) were added to 10 mL of the GO water dispersion under magnetic stirring at 500 rpm while kept at room temperature (25 °C) for two hours to yield the monolith precursor solution.

The monolith precursor mixture was then poured into molds of the desired shape, to fit the packed bed cartridge, and freeze-casted by exposing the mold's bottom surface to liquid nitrogen creating a temperature gradient (Fig. 1). The gradual growth of ice crystals is obtained in the monolith structure along the same axis. To achieve the maximum porosity, the approximate temperature gradient was about 2 °C.min <sup>-1</sup>, measured by infrared temperature gun [35]. The freeze-casted

monoliths were then lyophilized using a Labconco freeze dryer for 24 h.

The samples were coded based on their support (e.g., Pd@M for monolith and Pd@GO for 2D catalyst). In addition, their specific post synthesis treatment was included in the naming scheme. For example, Pd@M-MW is a Pd on GO monolith catalyst which is microwave treated.

# 2.3. Pd@M monolithic catalyst preparation

The procedure for the Pd@M monolithic catalyst preparation followed the GO monolith precursor preparation, but with the addition of a Pd precursor salt (PdCl $_2$  as the cationic, Pd(NH $_3$ ) $_4$ Cl $_2$  as the anionic salts) at 5 wt% metallic Pd with respect to GO, as well as ascorbic acid (2 M equivalence with respect to metallic Pd) were added to monolith mixture prior to the 2-hours esterification period. The Pd(NH $_3$ ) $_4$ Cl $_2$  and PdCl $_2$  were first dissolved in DI-water, and 0.1 M HCl aqueous solution, where PdCl $_4$   $^2$ – species were formed before addition to the GO monolith precursor solution.

Partial reduction of the monolith (and monolithic catalysts) was performed using ethanol vapor as the reducing agent in a closed round bottom flask heated to  $74\,^{\circ}\text{C}$  for  $2\,\text{h}$  (Fig. 1) located below the mold containing the monolith or monolith catalyst precursor solution. The treated monolith was then transferred to an autoclave reactor which was sealed and heated in an oven at  $100\,^{\circ}\text{C}$  for  $24\,\text{h}$ .

For comparison, in addition to Pd on GO monolith model sample prepared via use of  $PdCl_2$  precursor, a Pd on graphene oxide (GO) 2D catalyst was prepared via the identical reduction technique as the Pd@ M monolithic catalysts. However, the freeze casting and lyophilization steps were not applied for 2D catalysts.

# 2.4. Microwave-treatment

A microwave treatment was implemented to further reduce the Pd nanoparticles, improving their interaction with GO by formation of Pdgraphene defects inside the support structure [11]. The treatment was performed via a CEM Discover S microwave reactor by treating the sample at 100 °C for 1.5 min under varied power.

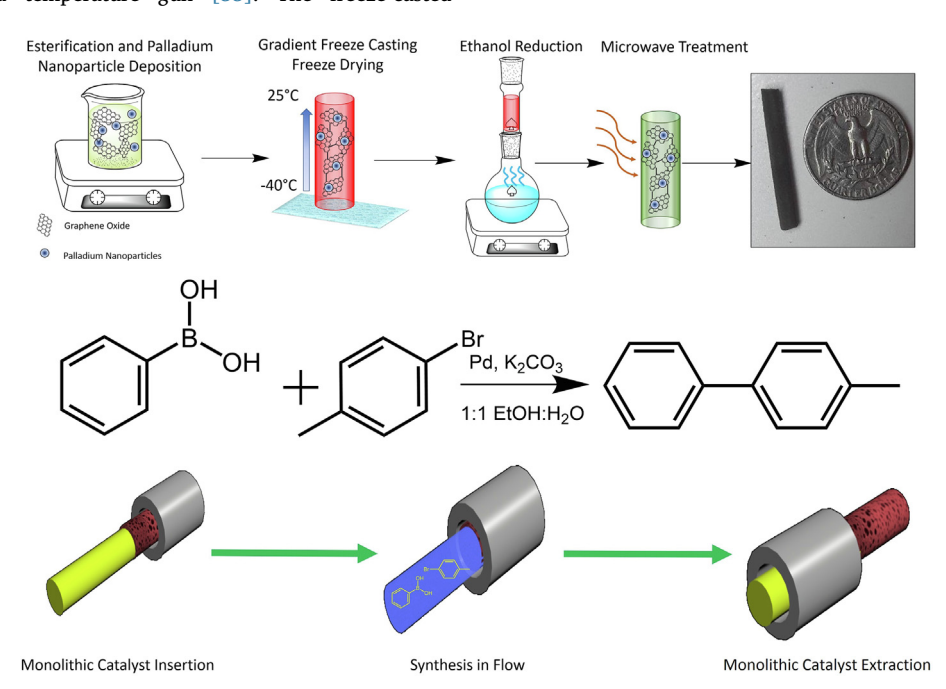


Fig. 1. The schematic illustration of monolithic catalyst preparation, the model Suzuki cross-coupling reaction, and the flow synthesis using the monoliths.

# 2.5. Micro CT-Scan imaging

The 3D micro CT scanning and imaging of the monoliths was performed using a Bruker Skyscan 1173 Micro-CT scanner. In order to obtain reliable maps, X-ray source potential was optimized at 130 kV, and exposure time for each image was set at 4000 ms. During the imaging, 360° rotation of specimen at 5 mm canonical distance from the source was maintained while random movements were not included. CTVOX free reconstruction software was used to process images. For all samples, green color was specifically assigned to the Pd particles captured in the 3D map, and the carbon-based matrix was colored white.

#### 2.6. Materials characterization

Scanning electron microscopy (SEM), X-ray diffraction analysis (XRD), and X-ray photoelectron spectroscopy (XPS), were done via a Hitachi SU-70 FE-SEM at 5 KV, a X'pert Pro PANanalytical XRD diffractometer (Cu K $\alpha$ ,  $\lambda=1.54$ Å, scanned from 5° to 85°) and a Thermo Fisher ESCALAB 250 X-ray spectrophotometer with 2 eV step for survey and 0.1 eV step for high resolution elemental scans, respectively. The XPS spectra were studied via CASAXPS 2.3 19PR software using NIST standard database 20 version 4.1 for detailed analysis.

High-resolution transmission electron microscopy (HR-TEM) on monolithic catalysts were conducted using an FEI Titan HR-TEM at 300 kV. The samples were prepared via drop-casting the monolith dispersions in methanol on carbon grids. The images could be found in supporting information (Section S. 4.).

BET Physisorption experiments were conducted for the 3D supports. The dried sample was massed and loaded into an analysis tube for degassing. The sample was degassed for 48 h at 250  $^{\circ}\text{C}$  under vacuum. Upon completion, the sample was massed prior to analysis. The analysis followed typical conditions for determining solid surface area by  $N_2$  isotherm adsorption.

The thermal behavior of the monolithic catalyst and GO were analyzed via differential scanning calorimetry (DSC). The experiment was conducted using a TA Instruments Q1000 DSC from  $-10\,^{\circ}\text{C}$  to  $350\,^{\circ}\text{C}$  to  $-10\,^{\circ}\text{C}$  at  $10\,^{\circ}\text{/min}$  heating/cooling rate under nitrogen gas atmosphere.

The palladium metal uptake was determined by first dissolving the sample in 1 vol/vol% hydrochloric acid solution for 24 h at  $25 \,^{\circ}\text{C}$ . Afterwards, the mixture was filtered using a  $0.2 \, \mu\text{m}$  syringe filter and ten times dilution with DI-water. Then the Pd concentration was measured using an inductively coupled plasma-optical emission spectroscopy (ICP-OES) (Agilent 5110 ICP-VCV-OES).

The average %Pd leached from the solid-supported catalysts were measured using the same ICP-VCV-OES device using the following protocol. At each 30-minute time point, 0.1 mL of the downstream was collected and mixed with 0.1 mL of 12.1 M HCl for acid digestion. After 20 times dilution with DI-water, the metal content was measured via ICP analysis. Afterwards, total leached Pd content was calculated using the following equation:

% leached  $Pd = (Pd \text{ conc. } (ppm) \times V_{passed}(L))/total Pd (mg) \times 100$ 

where the  $V_{passed}$  is the volume of passed liquid calculated based on the flow rate (0.01 L for each step). Then the average leached %Pd was calculated as the number average of each step's record. Remaining (or starting) Pd refers to the amount of retained (or starting) Pd on the catalyst.

# 2.7. Suzuki cross-coupling screening in flow

The Suzuki cross-coupling model reaction was investigated between 4-bromotoluene, and phenyl boronic acid (3.8 mmol) (0.08 and 0.0975 M, respectively) in a 40 mL mixture of ethanol-DI water (1:1), with potassium carbonate (0.24 M) to determine catalytic activity and longevity. The desired product was 4-phenyltoluene (Fig. 1). During

this process, a H-Cube mini flow reactor by ThalesNano® was used which contains a CatCart (ID:  $1.6\,\text{mm}$ , H: 7 mm) packed with either the 3D monolithic catalyst or the conventional 2D Pd@GO catalyst (28.6 µg calculated Pd in each CatCart) samples to be tested.

The continuous packed bed reactions were conducted at  $0.2\,\mathrm{mL.min}^{-1}$  flow rate and at 80– $90\,^{\circ}$ C. The reaction affluent mixture was collected at the reactor outlet in 30-minute time increments. An aliquot of each incremental collection vial was taken for analysis on GCMS after filtering with  $0.2\,\mu\mathrm{m}$  syringe filter and 10 times volumetric dilution with dichloromethane.

The confirmation of the product structure was obtained via 1H NMR analysis prepared and tested through the following procedure: First, the reaction effluent was diluted 3 times using ethyl acetate. After separation of the organic phase from the aqueous media, the supernatant organic phase was collected and dried using a rotary evaporator system. Finally, the dried product was dissolved in CDCl<sub>3</sub> for 1H NMR analysis. The analysis was conducted using a Bruker Ascend 600 NMR analysis instrument. The peak list of the product was: 4-Methylbiphenyl 1H NMR (600 MHz, CDCl<sub>3</sub>)  $\delta$  2.37 (s, 3H), 7.18–7.21 (m, 2H), 7.28–7.31 (m, 1H), 7.36–7.40 (m, 2H), 7.43 (d, J = 8.0 Hz, 2H), 7.52 (d, J = 7.0 Hz, 2H).

In order to remove the reaction residue from CatCarts, after each reaction, the whole system was purged with ethyl acetate, and a 1:1 ethanol:DI-water solution each for 10 min, respectively.

# 3. Results and discussion

Evaluation of the monolithic graphene-based nanosheets decorated with Pd catalysts consisted of material characterization, optimization of reaction temperature and microwave irradiation conditions, testing of catalytic performance, and development of a micro-CT mapping characterization technique was evaluated. The monolithic catalysts were characterized using X-ray photoelectron spectroscopy (XPS) to determine the oxidation state of Pd species and the catalysts were imaged using a scanning electron microscope (SEM). The effect of microwave treatment and reaction temperature on the monolith's catalytic performance were optimized to preserve the monolithic structure and enhance the catalytic performance, which was evaluated using Suzuki cross-coupling reaction as a model reaction. This model reaction was also used to evaluate the catalytic longevity of the 3D monolithic catalysts in comparison to the 2D catalyst packed bed. Finally, the micro-CT mapping was developed to provide a method of characterizing the Pd particle distribution throughout the monolith on a clear large-scale map.

# 3.1. X-ray photoelectron spectroscopy

According to the XPS spectra (Fig. 2), the oxygen content was significantly higher in monolithic catalysts compared to the 2D Pd@GO catalysts (Table 1). Since the reduction methods for both 3D and 2D catalysts were the same, the higher amount of detected oxygen was attributed to the functionalities contributing to the steric bond formation among the GO sheets. These detected oxygens are mostly found in forms of carboxylic and hydroxyl groups on the surface of GO which serve as water-compatible sites for the monolith. Therefore, the monolithic catalyst was more compatible with aqueous reaction media through the oxygen functional groups interactions with water. It is noteworthy that, the main effect of higher oxygen detected via XPS for monoliths is due to the steric bond formation among the GO sheets. Thus, it prevents the structure from collapsing under flow pressure of various solvent systems maintaining the 3D structure due to the steric cross-linking.

From the XPS survey quantification analysis on catalysts (Fig. 2A, C, E and G) no sulfur was detected at 162–170 eV binding energies, demonstrating the preparation method prevented sulfur-poisoning [36].

Based on previous reports, metallic Pd(0) and the ionic Pd(II) are

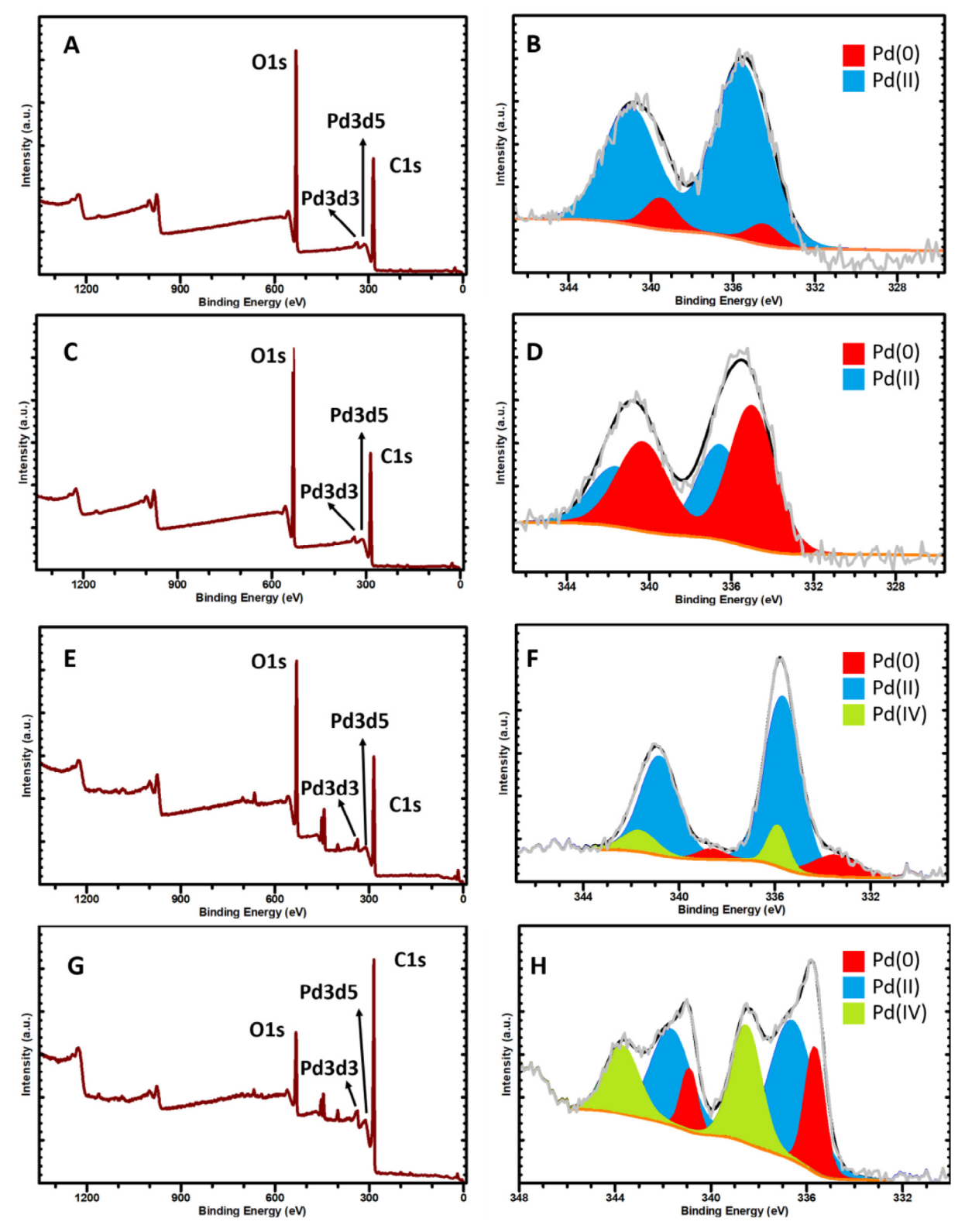


Fig. 2. XPS analysis of A, B) Pd@M-nonMW, C, D) Pd@M-MW, E, F) Pd@GO-nonMW, G, H) Pd@GO-MW.

mostly obtained species during the Pd catalyst immobilization on the solid support each of which proficiently catalyzes different reactions [37]. The detailed elemental analysis on Pd species revealed that the metallic species to total palladium species ratio in Pd@M (Fig. 2B), Pd@M- MW (Fig. 2D) monolithic catalysts and the 2D catalysts of Pd@GO (Fig. 2F, and Pd@GO-MW (Fig. 2H) were 34.2  $\pm$  5.4%, 65.1  $\pm$  7.6%, 19.4  $\pm$  3.7% and 32  $\pm$  3.9%, respectively. Based on

the catalytic cycle for a Suzuki cross-coupling reaction [38], the catalytic species readily contributing to the process are metallic Pd species. Hence, it is confirmed that the fraction of metallic Pd is one of the factors corresponding to the catalytic activity of a solid-supported catalyst in a direct fashion but not the only one as previously discussed. Hence, a catalyst with more Pd(0) is expected to have higher catalytic activity. From the synthetic chemistry perspective, as shown in the

Table 1
Catalyst system oxygen and palladium contents as well as operating backpressure and lifetime in flow chemistry.

Catalyst System	Oxygen content (wt%)*	Palladium content (wt%)§	Backpressure (PSI)	Lifetime (min)	TON (Average @ > 20% conversion)	Average %Pd leached every 30 min §	Total %Pd leached §
Pristine GO Monolith	39.17	_	_	_	-	-	-
Pd@M-non MW	23.73	3.79	0	330	3591	$1.11 \pm 0.54$	$11.6 \pm 2.3$
Pd@M-MW	19.46	4.45	0	120	2340	$2.64 \pm 1.39$	$19.9 \pm 3.4$
Pd@M (PdCl2)-MW	20.31	3.29	1	60	1671	$9.72 \pm 2.34$	$33.1 \pm 6.6$
Pd@GO-non MW	28.71	2.86	4	120	2088	$13.46 \pm 2.89$	$51.2 \pm 14.7$
Pd@GO-MW	14.19	3.16	4	90	76	$11.97 \pm 3.11$	$47.5 \pm 9.2$

- \* Measured by XPS analysis.
- § Measured by ICP-OES.

Fig. 2, Pd@M-MW should have the highest activity since the majority of Pd particles in that monolithic catalyst are metallic Pd species. However, to have a comprehensive and realistic understanding of the catalytic activities, other process engineering challenges have to be considered. For instance, differences in the mechanical sturdiness of these 3D structures while used in flow can have adverse effects on the overall catalytic activity as well as longevity of the monolithic catalysts.

The significant difference among the monolithic catalysts and 2D Pd@GO catalysts recorded via XPS was that a palladium (IV) (Pd(IV)) species was detected in Pd@GO and Pd@GO-MW catalysts (Fig. 2F and H, respectively) while such species was absent in monoliths. Due to the oxide species formation, a longer reductive pretreatment activation (initial transformation of all Pd species to Pd(0)) was needed before performing the Suzuki cross-coupling reaction. The reason for the increase in Pd(IV) fraction from 9% to 22% based on relative peak area could be attributed to the smaller particle size of the Pd(II) and Pd(0) species not masking the Pd(IV) species thus expressing the Pd(IV) peak more strongly in the microwave-treated catalyst compared to the asprepared one [39].

# 3.2. Suzuki cross-coupling catalytic activity and catalyst lifetime analysis in flow

The model Suzuki reaction chosen for testing of the catalyst performance was the C–C bond formation between 4-bromotoluene and phenylboronic acid, detailed in Fig. 1 and the methods section. In order to systematically optimize the monolithic catalyst synthesis conditions for optimal material performance in continuous catalysis various parameters were studied. The effect of Pd precursor used in catalyst synthesis, as well as the effect of reaction temperature during the first 60 min of the reaction in flow was studied (Fig. 3A & B, respectively).

Use of different palladium precursors, PdTA and PdCl<sub>2</sub>, were first investigated using the model Suzuki reaction (Fig. 3 A). The Pd@M (PdCl<sub>2</sub>)-MW deactivation was recorded to be two times earlier than the Pd@M-MW entry. Hence the monolithic catalysts prepared using PdTA were more catalytically active and durable than materials prepared using PdCl<sub>2</sub>.

The catalytic activity drastically decreased at  $90\,^{\circ}\text{C}$  reaction temperature for the monolithic catalysts (Fig. 3 B). This loss in activity was related to the thermal decomposition of the ester bonds, causing the monolith to collapse and thus hinder mass transfer.

The 2D catalysts (Pd@GO and Pd@GO-MW) and 3D monolithic catalysts (Pd@M and Pd@M-MW) were next investigated for catalyst lifetime in continuous packed bed configuration (Fig. 3C). Most notably the 3D monoliths, particularly Pd@M, had better catalyst performance with respect to catalyst lifetime. The rapid completion of the cross-coupling reaction by Pd@M within the first 5 min of reagent passage (prior to physical deactivation) signified the advantage of the proposed EtOH-assisted deposition method in preparation of highly active Pd particles. Longer reaction times at similar cross-coupling reaction conditions were reported for other Pd preparation techniques such as conventional hydrazine [40] and hydrogen gas [41] (Table 2).

According to XPS analysis, Pd@M-MW contained almost 2 times Pd(0) species content compared to Pd@M. The Pd(0) content as the reported effect of microwave treatment on Pd particle anchoring and activity increase [11] were attributed to the higher initial activity over the nonmicrowaved monolithic catalyst. As it is also shown in Fig. 3C of the manuscript, the initial (during the first hour of flow reaction) catalytic activity of microwave-treated monolith (higher metallic Pd) is noticeably higher than the non-treated one. However, the activity is then drastically reduced shortly after the mentioned period due to physical deactivation. This deactivation is a sign that another factor, such as accessibility of the reagents to the active sites (metallic Pd surfaces), plays an essential role in the catalytic activity. Therefore, it could be concluded that during the first hour of flow reaction when the microwave-treated monolith's active sites were physically accessible, its catalytic activity was significantly higher than the non-treated counterpart. However, the Pd@M outperformed the Pd@M-MW from the longevity perspective which was attributed to the defects or holes created by microwave irradiation decreasing the structural integrity of the monolith. The abrupt collapse of the monolith into a highly packed single piece was the reason for the observed deactivation of the MWtreated monolithic catalyst (Pd@M-MW), thus resulting in drastically reduced catalytic activity.

The backpressure of all materials was important to measure as an ideal packed bed configuration will have minimal backpressure across the packed column. No backpressure was recorded for the Pd@M monolithic catalyst during the reaction indicating this material was more suitable for flow chemistry compared to the 4-bar backpressure of the conventional 2-D catalyst. This advantage enabled uniform flow rate through the reactor as well as higher overall throughput, potentially improving the process economy.

The other significant advantage of the monolithic over conventional 2D Pd@GO catalysts was demonstrated by a Pd leaching study (Table 1). It was determined that for every 30 min of operation, almost over 12% of Pd is leached off from the 2D Pd@GO catalysts into the reaction media. Compared to the 2D Pd@GO catalyst, the amount of Pd leached was significantly reduced 4 fold with the monolithic catalyst.

Table 2 shows the comparison between previous reports of the same Suzuki cross-coupling reaction in flow between the Pd@M and other catalysts. Notably, the prepared Pd@M catalyst doesn't require a diluent, such as glass beads, due to their customizability and flexibility of shape design. The monolithic catalysts effectively outlive the conventional catalysts and maintain higher activity and physical integrity at elevated temperatures.

As shown in Greco et al.'s work on Suzuki reactions in flow [3], packed beds of Pd(0) catalysts struggle to maintain conversion above 30% throughout the first hour of the process. However, Pd@M monolithic catalysts demonstrated over 70% average conversion during that same period (Fig. 3C). Maintaining high activity over 5 h reliably, the superior longevity and sustainability of monolithic Pd@M catalysts over previously reported catalyst packed beds can be assured.

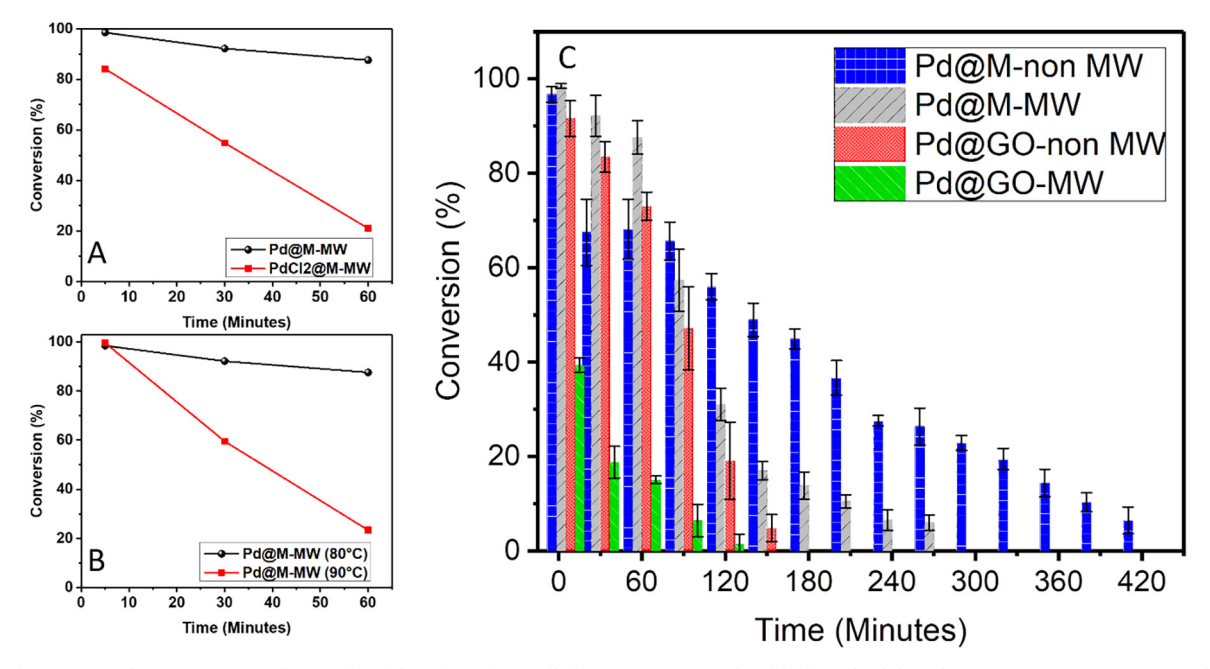


Fig. 3. Suzuki cross-coupling screening in flow study of the effect of A) Palladium precursors (PdTA-black, and PdCl<sub>2</sub>-red), B) reaction temperature, and C) various catalyst materials. All the reactions were conducted at  $0.2 \, \text{mL.min}^{-1}$  and  $80 \, ^{\circ}\text{C}$  (except Fig. 3 B) and the selectivity towards the desired product was greater than 95%.

# 3.3. Electron microscopy and structural analysis

Scanning electron microscopy revealed interesting differences in the Pd particle size and distribution as well as the microstructure of the different 2D Pd@GO and 3D Pd@M catalysts prepared using both chemical (vitamin C) and microwave irradiation reduction steps (Fig. 4). The average Pd particle size of the 2D Pd@GO and Pd@GO-MW catalysts (Fig. 4A and B) were  $36.8 \pm 6.2$  and  $28.3 \pm 4.5$  nm, respectively. In contrast the Pd particle size of the 3D monolithic catalysts, Pd@M and Pd@M-MW, were  $27.8 \pm 2.8$  nm and  $18.5 \pm 1.2$ , respectively (Fig. 4C and D), which was also confirmed by HR-TEM imaging (see supporting information, Section S. 4). Based on these size measurements it is thought that the potential active surface area of Pd nanoparticles for catalytic activity was higher in the monolithic catalyst samples and more so in MW entries which consist of smaller Pd particles.

The HR-TEM imaging of the monolithic catalysts (supporting information Figure S. 4.) revealed that the cubic close-packed (CCP) structure of Pd particles was not changed by the treatment. The d-spacing of the mentioned particles was slightly increased due to the treatment (see Section S. 4 in supporting information).

According to the International Union of Pure and Applied Chemistry (IUPAC)'s classification of porous structures [44], and based on the electron microscopy (Fig. 4, and S. 4), the monolithic catalysts could be

categorized as nanoporous structures, mostly identified in the mesopore range. The specific surface area measurement of the monolithic catalysts via nitrogen physisorption technique was attempted multiple times using various methodologies (See Section S. 2 in the supporting information). However, the results were inconclusive. The DSC analysis (see Section S. 5 in supporting information) showed that the entrapped water in these hybrid systems, absorbed by PVA, could be considered as an integral part of the structure, which its removal leads to a significant change in the structure. Therefore, performing gas adsorption analyses at elevated temperatures, should it be feasible at all, could not be considered as a realistic and reliable representative of the actual material's properties.

Another important characteristic revealed by electron microscopy was physical evidence of defects in the support structure resulting from MW irradiation treated catalyst compared to the as-prepared one. These hole-like defects formed within the GO sheets during microwave irradiation due to extremely high and localized temperatures surrounding the forming Pd nanoparticles during reduction [45]. These graphene holes or defects supporting Pd have been demonstrated to provide enhanced catalytic activity of solid-supported catalysts through tow mechanisms [11,15,46,47]. Firstly, through this phenomenon new defects are introduced to the graphene structure which are known to act as active sites for metal catalytic applications. Secondly, since the Pd particles are embedded inside the holes, the particles are more tightly

**Table 2**The comparison between the previous Pd catalyzed Suzuki cross-coupling reactions in flow and the current study.

Catalyst (mol% Pd)	Temperature (°C)	Reactor (minute residence time)	Flow rate (mL.min <sup>-1</sup> )	1st hour average conversion (GC RPA%)	Refs.
Pd on Polyurea (–)	55	HPLC column packed bed (4)	0.2	100	[42]
Pd on Fibercat (-)	120	X-Cube (3)	0.155	30	[3]
Pd@MIL-101-NH <sub>2</sub> MOF (w/glass beads) (1)	50	House-made Packed bed (35–40)	0.05	94	[43]
Pd on CuO* (1)	80	Batch (10)	_	~88	[40]
Pd on γ-Alumina <sup>§</sup> (0.5)	60	Batch (24 hrs)	_	~65	[41]
Pd@M-MW (0.5)	80	H-Cube mini (7)	0.2	93	This study

<sup>\*</sup> Deposition via hydrazine.

<sup>§</sup> Deposition via H<sub>2</sub> gas.

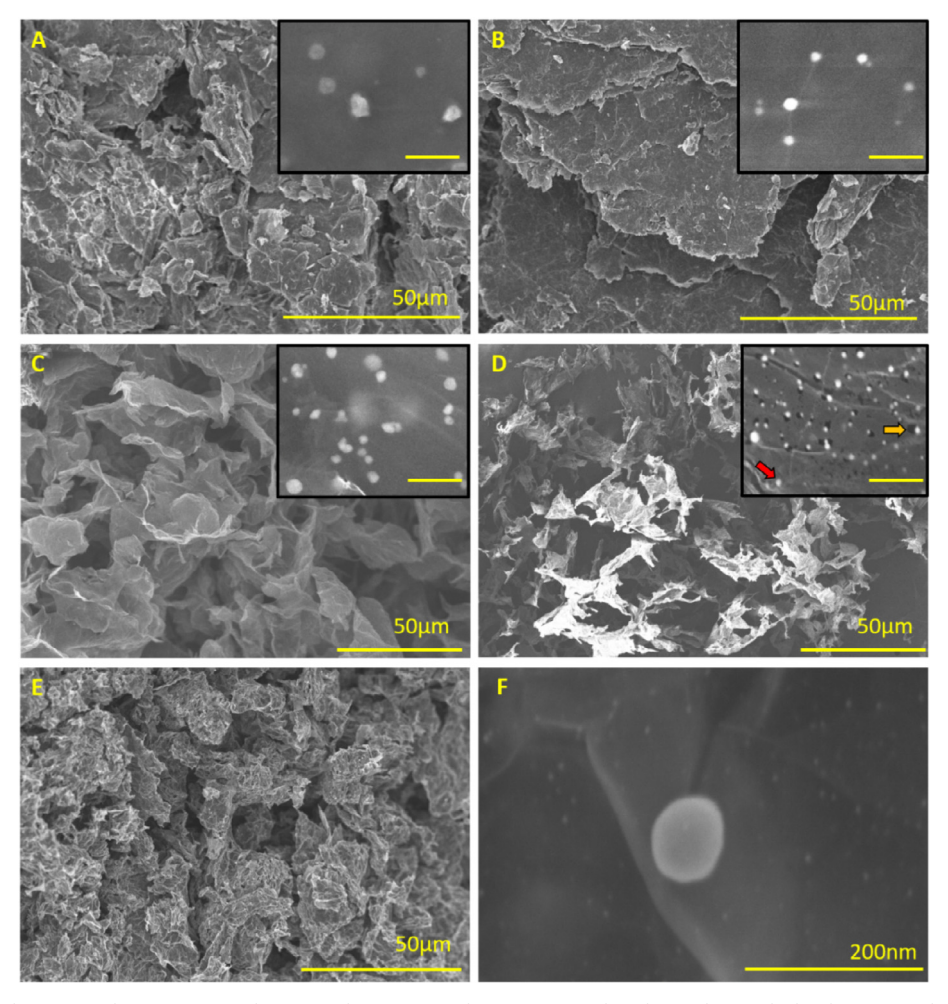


Fig. 4. SEM images of A) Pd@GO, B) Pd@GO-MW, C) Pd@M, D) Pd@M-MW (in the inset image: the Pd particles are the bright spots, and the holes into graphene are the dark spots, indicated by the red and yellow arrows, respectively.), and E, and F) overall porous structure and particle imaging (incorporating sub 10 nm and over 100 nm particles) of Pd@M after the reaction, respectively. The inset image scale bars are 50 nm.

bound and have a stronger electronic connection with the support. Hence, the Pd leaching is minimized while charge transfer capabilities of the whole catalyst system necessary for performing the catalytic cycle's redox reactions are significantly improved. Thus, the formation of holes is considered among the crucial phenomena required for having a highly active catalyst. However, in monolithic materials these defects could result in reduced mechanical stiffness. Therefore, the formation of these holes needs to be optimized to provide enhanced catalytic performance while also retaining the mechanical and structural properties of monolith materials required for use in continuous flow reactions.

The comparison between the Pd particle size distribution before and after reaction (Fig. 4C, and F) showed that in Pd@M catalyst the average particle size after Suzuki cross-coupling flow synthesis was increased to  $30.6 \pm 11.7\,\mathrm{nm}$ . The significantly higher standard deviation value is due to the formation of larger Pd particles (>  $100\,\mathrm{nm}$ ). The post-reduction of Pd(II) particles to Pd(0) via electron donation from GO monolith to the Pd particles during the reaction could be the responsible phenomenon for such aggregation.

The microstructure of Pd@M monolithic catalyst before and after flow (Fig. 4C, and E, respectively) also revealed that while the macroporous structure of the monolith was preserved, the micropores were filled with organic compound crystal residue, indicating that mass transfer deactivation was one of the effects playing an important role in the lifetime of the monolith. Additionally, the partially insoluble crosscoupling product residue on the monolithic catalyst structure, resulting

in Pd particle-poisoning and deactivation.

# 3.4. Computed tomographic (CT) scan mapping of monolithic catalysts

In order to properly characterize the Pd decorated 3D monolithic structure, a macroscopic characterization technique is needed to evaluate the distribution of Pd throughout the entire monolith material. Therefore, micro CT-mapping was investigated as a new technique to provide this characterization. Micro CT-mapping is applicable because such imaging is based on the intensity of diffracted X-rays. More specifically, two main factors provide resolution between Pd and graphene final images: atomic number of constituent elements and the crystallinity of the materials. The heavier Pd atoms and their highly crystalline structures result in higher X-ray diffraction in comparison to the carbon of GO. This difference in X-ray diffraction provided the necessary resolution and contrast to distinguish the two materials and therefore the distribution of Pd throughout the GO monolith. In addition, the opacity of the 3D image can give an indirect measurement of the porosity of the structure which was important in qualitatively evaluating the monolith for use in continuous packed bed reactors. This indirect macroscopic characterization of structure was significant in evaluating porosity before and after reactions since complete solvent elimination was technically difficult. Consequently, surface area analysis via conventional methods (such as physisorption techniques) were not possible on 'wet' materials. The micro-CT scan analyses of the 3D monolithic catalysts, Pd@M and Pd@M-MW, show that a relatively uniform distribution of

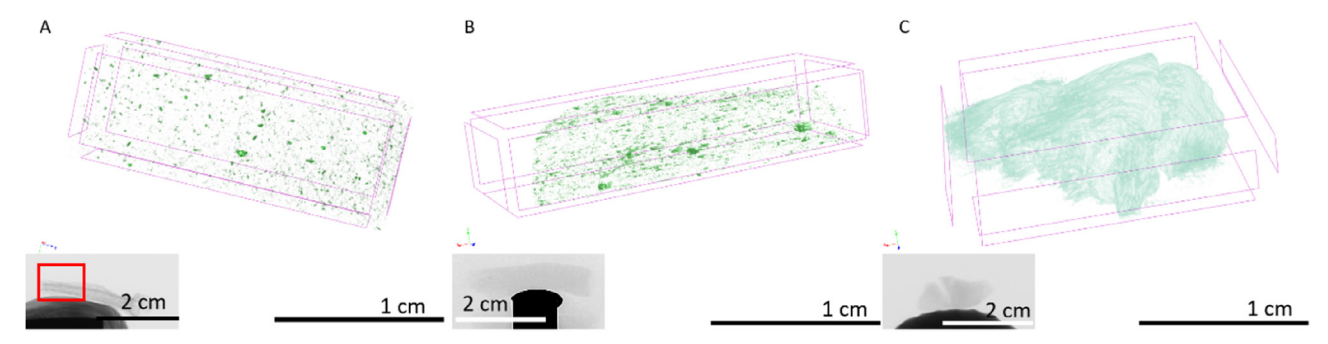


Fig. 5. Micro-CT analysis of A) Pd@M-MW, B) Pd@M-non MW, and C) Pd@M-non MW after flow reaction.

Pd particles were achieved throughout the entire monolith structure. (Fig. 5A and B). Micro-CT mapping also reveals the density of Pd detected is slightly lower in non-treated monolithic catalyst (Fig. 5B). This result was consistent with lower Pd uptake of Pd@M compared to Pd@ M-MW (Table 1) as determined by ICP-OES.

The micro-CT characterization was also exceptionally useful in analyzing pre and post-reaction effects on the monolith materials. A section of reacted monolith in flow was characterized (Fig. 5C). The drastic change in contrast between Fig. 5B and C, particularly the opacity and texture of the obtained image, indicates that a significant amount of X-ray diffraction was detected in this specimen. The two possible hypotheses for the observation are: the geometrical diffraction caused by physical deactivation and collapse of porous structure of the monolith, and/or the entrapment of crystallized 4-phenyltoluene as well as 4-bromotoluene (Fig. 1) inside the structure. The first hypothesis was less likely as the SEM imaging showed that the porous structure was preserved through the flow synthesis (Fig. 4E). The electron microscopy technique also revealed that the texture of graphene nanosheets was altered after the reaction as they were covered with a crystalline residue. Therefore, the bulky, and opaque 3D image of monolith obtained via micro-CT technique gives a clear indication that micropores of the structure was filled with reaction product residue, which was confirmed by the SEM technique.

The further ICP-OES analysis on the effluent from the final rinse of the cartridges with ethyl acetate, removing the entrapped organic crystals, showed that both in monolithic and 2D catalysts, the entrapped crystals contained less than 1% (0.003, and 0.028 mg, respectively) of the total Pd loading in the cartridges (26 mg). This observation confirmed that the entrapped Pd was negligible to the overall leached metal. Therefore, limited to no activity from such metallic species could be expected.

# 4. Concluding remarks

A state of art, all aqueous method for preparation and non-destructive analysis of palladium @ graphene monolithic catalysts was developed and systematically studied. The proposed route in this work it is the result of the optimized monolithic catalyst pursuing high catalytic activity as well as long lifetime for Suzuki cross-coupling model reaction in flow.

In addition to the higher activity obtained from PdTA-based monoliths compared to PdCl<sub>2</sub>-based catalysts, it was shown that microwave treatment can have noticeable effects on these hybrid materials performances

The ICP-OES results recorded slightly higher Pd uptake in MW-treated monoliths. However, by XPS analysis it was shown that the majority of Pd species in those catalysts were Pd(II), requiring initial activation prior to contributing into the Suzuki catalytic cycle.

Nevertheless, according to both reaction screening, the MW-treated monoliths collapsed in a faster pace compared to non-MW treated entries, leading to lower catalytic lifetime.

The longevity, and backpressure of the monoliths in flow were compared to 2D Pd @ graphene oxide catalyst packed beds. Significant improvements in both characteristics were recorded for 3D monolithic catalysts. Specifically, a 300% increase in longevity of monolithic catalysts compared to 2D catalysts was of great importance.

The scanning electron microscopy of monolithic catalysts showed that the average Pd particle size distribution went through a significant change during the flow chemistry. The formation of particles with over 200 nm diameter in MW-treated monoliths after flow, was thought to be the result of Pd(II) to Pd(0) post-reduction phenomena. Hence, correlating closely with elemental analysis conducted via XPS.

Finally, the proof of concept for preparation of a model structure for large-scale elemental analysis of micro-CT was successfully demonstrated as both Pd particle distribution as well as porosity studies on monolithic catalysts were reported.

The 3D map of Pd particles distribution throughout the monolith can provide valuable information not only from experimental optimization perspective, but also as a reference model to be used for further computational studies on solid-supported flow catalysis.

# **Declaration of Competing Interest**

The authors declare that they have no known competing financial interests or personal relationships that could have appeared to influence the work reported in this paper.

# Acknowledgements

Authors would like to thank Dr. Hu Yang and Dr. Xuejun Wen for providing access to the lyophilizing equipment as well as the financial support from the National Science Foundation Industry/University Collaborative Research Center Grant (IIP 1464595).

# Appendix A. Supplementary data

Supplementary data to this article can be found online at https://doi.org/10.1016/j.cej.2019.122598.

# References

- W. Jerdan, Practical and Experimental Chemistry: adapted to Arts and Manufactures, H. Colburn, London, 1838 392-392.
- 2] J.A. Moulijn, P.W.N.M. van Leeuwen, R.A. van Santen (Eds.), Chapter 1 History of catalysis, in Studies in Surface Science and Catalysis, Elsevier, 1993, pp. 3–21.
- [3] R. Greco, et al., Benchmarking immobilized di- and triarylphosphine palladium catalysts for continuous-flow cross-coupling reactions: efficiency, durability, and metal leaching studies, ACS Catal. 5 (2) (2015) 1303–1312.
- [4] T. Noël, et al., Palladium-catalyzed amination reactions in flow: overcoming the challenges of clogging via acoustic irradiation, Chem. Sci. 2 (2) (2011) 287–290.
- [5] J. Wisniak, The history of catalysis: from the beginning to nobel prizes, Educación química 21 (1) (2010) 10.
- [6] J. Pritchard, et al., Heterogeneous and homogeneous catalysis for the hydrogenation of carboxylic acid derivatives: history, advances and future directions, Chem. Soc. Rev. 44 (11) (2015) 3808–3833.
- [7] T.N. Glasnov, S. Findenig, C.O. Kappe, Heterogeneous versus homogeneous

- palladium catalysts for ligandless Mizoroki-Heck reactions: a comparison of batch/microwave and continuous-flow processing, Chem. Eur. J. 15 (4) (2009)
- [8] Administration, U.F.a.D., Q3D elemental impurities guidance for industry, 2015.
- R.E.Y. Eaton, Synthesis Gas Conversion with ZSM-5 Supported Ruthenium Catalysts, Virginia Commonwealth University, Dept. of Chemistry, 1983.
- [10] S. Chen, X. Chen, H. Zhang, Nanoscale size effect of octahedral nickel catalyst towards ammonia decomposition reaction, Int. J. Hydrogen Energy 42 (27) (2017) 17122–17128.
- [11] S.E. Gilliland, et al., Electrostatic adsorption-microwave synthesis of palladium nanoparticles on graphene for improved cross-coupling activity, Appl. Catal. A 550 (2018) 168–175.
- [12] X. Song, et al., Eco-friendly controllable synthesis of highly dispersed ZIF-8 embedded in porous Al2O3 and its hydrogenation properties after encapsulating Pt nanoparticles, Appl. Catal. B 227 (2018) 13–23.
- [13] L. Işıkel Şanlı, et al., Engineered catalyst layer design with graphene-carbon black hybrid supports for enhanced platinum utilization in PEM fuel cell, Int. J. Hydrogen Energy 42 (2) (2017) 1085–1092.
- [14] L.I. Şanlı, et al., Development of graphene supported platinum nanoparticles for polymer electrolyte membrane fuel cells: effect of support type and impregnation-reduction methods, Int. J. Hydrogen Energy 41 (5) (2016) 3414–3427.
- [15] Y. Yang, et al., Three dimensional composites of graphene as supports in Pd-catalyzed synthetic applications, React. Chem. Eng. (2018).
- [16] M.J. Ahmed, A.A.H. Kadhum, Hydrogenation of d-fructose over activated charcoal supported platinum catalyst, J. Taiwan Inst. Chem. Eng. 42 (1) (2011) 114–119.
- [17] S. Palanisamy, et al., Palladium nanoparticles decorated on activated fullerene modified screen printed carbon electrode for enhanced electrochemical sensing of dopamine, J. Colloid Interface Sci. 448 (2015) 251–256.
- [18] H.K. Potukuchi, A.P. Spork, T.J. Donohoe, Palladium-catalyzed -arylation of carbonyls in the de novo synthesis of aromatic heterocycles, Org. Biomol. Chem. 13 (15) (2015) 4367–4373.
- [19] M. Li, et al., Palladium-catalyzed C H arylation of α, β-unsaturated imines: catalyst-controlled synthesis of enamine and allylic amine derivatives, Angew. Chem. Int. Ed. 55 (8) (2016) 2825–2829.
- [20] D.A. Graf von der Schulenburg, M.L. Johns, Catalyst effectiveness factor distributions in isothermal packed bed reactors, Chem. Eng. Sci. 66 (13) (2011) 3003–3011.
- [21] M.R. Rahimpour, et al., Methanol synthesis in a novel axial-flow, spherical packed bed reactor in the presence of catalyst deactivation, Chem. Eng. Res. Des. 89 (11) (2011) 2457–2469.
- [22] P. He, et al., Scaling up of continuous-flow, microwave-assisted, organic reactions by varying the size of Pd-functionalized catalytic monoliths, Beilstein J. Org. Chem. 7 (2011) 1150–1157.
- [23] F. Liguori, et al., Unconventional Pd@Sulfonated silica monoliths catalysts for selective partial hydrogenation reactions under continuous flow, ChemCatChem 9 (16) (2017) 3245–3258.
- [24] L. Minati, et al., Palladium nanoparticle functionalized graphene xerogel for catalytic dye reduction, Dalton Trans. 47 (41) (2018) 14573–14579.
- [25] A. Modak, A. Bhaumik, Surface-exposed Pd nanoparticles supported over nanoporous carbon hollow tubes as an efficient heterogeneous catalyst for the CC bond formation and hydrogenation reactions, J. Mol. Catal. A: Chem. 425 (2016) 147–156.
- [26] A.S. Díaz-Marta, et al., Three-dimensional printing in catalysis: combining 3D heterogeneous copper and palladium catalysts for multicatalytic multicomponent reactions, ACS Catal. 8 (1) (2018) 392–404.
- [27] S. Cai, et al., Porous Ni-Mn oxide nanosheets in situ formed on nickel foam as 3D hierarchical monolith de-NOx catalysts, Nanoscale 6 (13) (2014) 7346–7353.

- [28] S. Mukdasai, et al., Electrodeposition of palladium nanoparticles on porous graphitized carbon monolith modified carbon paste electrode for simultaneous enhanced determination of ascorbic acid and uric acid, Sens. Actuat. B Chem. 218 (C) (2015) 280–288.
- [29] A.V. Nakhate, G.D. Yadav, Palladium nanoparticles supported carbon based graphene oxide monolith as catalyst for sonogashira coupling and hydrogenation of nitrobenzene and alkenes, Chem. Select 1 (13) (2016) 3954–3965.
- [30] Y. Fam, et al., Correlative multiscale 3D imaging of a hierarchical nanoporous gold catalyst by electron, ion and X-ray nanotomography, ChemCatChem 10 (13) (2018) 2858–2867.
- [31] M.T. Kreutzer, et al., Monoliths as biocatalytic reactors: smart gas liquid contacting for process intensification, Ind. Eng. Chem. Res. 44 (25) (2005) 9646–9652.
- [32] S.C. Garcea, Y. Wang, P.J. Withers, X-ray computed tomography of polymer composites, Compos. Sci. Technol. 156 (2018) 305–319.
- [33] L. Li, Modeling of fatigue hysteresis behavior in carbon fiber-reinforced ceramic-matrix composites under multiple loading stress levels, J. Compos. Mater. 51 (7) (2017) 971–983.
- [34] S. Ghobadi, et al., Graphene-reinforced poly(vinyl alcohol) electrospun fibers as building blocks for high performance nanocomposites, RSC Adv. 5 (103) (2015) 85009–85018.
- [35] O.T. Picot, et al., Using graphene networks to build bioinspired self-monitoring ceramics, Nat. Commun. 8 (2017) 14425.
- [36] B. Quan, et al., Single source precursor-based solvothermal synthesis of heteroatom-doped graphene and its energy storage and conversion applications, Sci. Rep. 4 (2014) 5639.
- [37] T. Ghosh, et al., Benign approach for methyl-esterification of oxygenated organic compounds using TBHP as methylating and oxidizing agent, Appl. Catal. B 226 (2018) 278–288.
- [38] N. Miyaura, T. Yanagi, A. Suzuki, The palladium-catalyzed cross-coupling reaction of phenylboronic acid with haloarenes in the presence of bases, Synth. Commun. 11 (7) (1981) 513–519.
- [39] M.C. Militello, S.J. Simko, Palladium Oxide (PdO) by XPS, Surf. Sci. Spectra 3 (4) (1994) 395–401.
- [40] H.A. Elazab, M.A. Sadek, T.T. El-Idreesy, Microwave-assisted synthesis of palladium nanoparticles supported on copper oxide in aqueous medium as an efficient catalyst for Suzuki cross-coupling reaction, Adsorpt. Sci. Technol. 36 (5–6) (2018) 1352–1365.
- [41] F. Ulusal, et al., Supercritical carbondioxide deposition of γ-Alumina supported Pd nanocatalysts with new precursors and using on Suzuki-Miyaura coupling reactions, J. Supercrit. Fluids 127 (2017) 111–120.
- [42] C.K.Y. Lee, et al., Efficient batch and continuous flow Suzuki cross-coupling reactions under mild conditions, catalysed by polyurea-encapsulated palladium (ii) acetate and tetra-n-butylammonium salts. Chem. Commun. 16 (2005) 2175–2177.
- [43] V. Pascanu, et al., Highly functionalized biaryls via suzuki-miyaura cross-coupling catalyzed by Pd@MOF under batch and continuous flow regimes, ChemSusChem 8 (1) (2015) 123–130.
- [44] M. Nasrollahzadeh, Chapter 2 types of nanostructures, in: M. Nasrollahzadeh (Ed.), Interface Science and Technology, Elsevier, 2019, pp. 29–80.
- [45] K. Savaram, et al., Dry microwave heating enables scalable fabrication of pristine holey graphene nanoplatelets and their catalysis in reductive hydrogen atom transfer reactions. Carbon 139 (2018) 861–871.
- [46] A.R. Siamaki, et al., Microwave-assisted synthesis of palladium nanoparticles supported on graphene: a highly active and recyclable catalyst for carbon-carbon cross-coupling reactions, J. Catal. 279 (1) (2011) 1–11.
- [47] Y. Yang, et al., More than just a support: graphene as a solid-state ligand for palladium-catalyzed cross-coupling reactions, J. Catal. 360 (2018) 20–26.